

# Single InGaAs Quantum Dot Coupling to the Plasmon Resonance of a Metal Nanocrystal

A. Urbańczyk · G. J. Hamhuis · R. Nötzel

Received: 24 June 2010 / Accepted: 9 September 2010 / Published online: 28 September 2010  
© The Author(s) 2010. This article is published with open access at Springerlink.com

**Abstract** We report the observation of coupling of single InGaAs quantum dots with the surface plasmon resonance of a metal nanocrystal, which leads to clear enhancement of the photoluminescence in the spectral region of the surface plasmon resonance of the metal structures. Sharp emission lines, typical for single quantum dot emission, are observed, whereas for reference samples, only weak continuous background emission is visible. The composite metal–semiconductor structure is prepared by molecular beam epitaxy utilizing the principle of strain-driven adatom migration for the positioning of the metal nanocrystals with respect to the quantum dots without use of any additional processing steps.

**Keywords** Quantum dots · Surface plasmon resonance · InAs · Photoluminescence · In nanocrystals

## Introduction

Manipulation of the properties of single quantum emitters is an important topic of current research. It has been traditionally achieved in various systems by coupling of the emitter to a cavity [1–3]. Recently, there is an increasing interest in achieving this goal by coupling the emitter to metal nanostructures that act as an optical analog of an antenna at radiofrequencies [4]. Quantum dots (QDs) are an important class of quantum emitters as they can have engineered optical response. Composite metal–semiconductor

QD structures enable even more control over the optical properties. The controllable properties include radiative lifetime, absorption cross-section and nonlinear susceptibility [5, 6]. Controlling them is not only of interest in the context of basic science, but also has numerous applications. The most obvious are increasing the efficiency of light emitters, detectors and solar cells. Apart from that, metal optics or plasmonics enables confinement of light at truly sub-wavelength scales. Combining metal nanostructures with active materials can lead to ultimate scaling down of coherent light sources and other active devices, which could be potentially used for ultra-fast, nanoscale photonic integrated circuits that could compete with their electronic counterparts [7, 8].

Other very interesting applications are in miniaturization of quantum functional devices, such as single or entangled photon sources [2, 9]. Such applications require coupling of a single quantum emitter to a metal nanostructure. This is not an easy task, because it requires extremely precise control over the mutual position and separation of the emitter and the metal nanostructure. This is crucial, as too small separation will result in quenching of the emitter due to nonradiative recombination at the metal interface and too large separation will cause, that the plasmonic effects will be negligible [5]. That is why truly nanometer scale precision is required, which rules out usage of all top-down fabrication approaches and leaves only bottom-up processes. In case of colloidal QDs, chemical self-assembly based on long organic molecules that bind to the functionalized surface of a metal nanoparticle is often used [10]. Also for solid-state systems such as molecular beam epitaxy (MBE) grown InGaAs/GaAs QDs, a very promising approach exists, which is based on strain-driven adatom migration. So far, it was mostly used for forming complex semiconductor nanostructures like QD molecules or for

---

A. Urbańczyk (✉) · G. J. Hamhuis · R. Nötzel  
COBRA Research Institute on Communication Technology,  
Department of Applied Physics, Eindhoven University  
of Technology, 5600 MB Eindhoven, The Netherlands  
e-mail: A.J.Urbanczyk@tue.nl

positioning of QDs on strain-engineered substrates [11, 12]. It has been demonstrated that the same principle works also for the alignment of metal nanocrystals on top of QDs, provided that the metal recognizes the underlying crystalline structure of the substrate [13]. Since the present-day MBE technology offers very precise control of growth rates and other deposition parameters, strain-driven migration can be used for extremely precise lateral and vertical positioning of metal nanocrystals with respect to underlying QDs, which allows full utilization of the plasmonic effects.

In this article, we report the observation of coupling of single near-surface InGaAs QDs with the surface plasmon resonance (SPR) of an In nanocrystal. Micro-photoluminescence (micro-PL) measurements at low temperature reveal intense sharp lines due to single QD emission in the spectral region of the SPR. Reference samples with no In nanocrystals measured under the same conditions reveal only a much weaker broad background emission. Thus, absolute QD emission efficiency enhancement due to coupling to the In SPR is observed proving that the In nanocrystals act as efficient nanoantennae. The In nanocrystals are aligned on top of the QDs using the principle of strain-driven adatom migration, which enables precise control over the QD–metal separation.

## Experimental Details

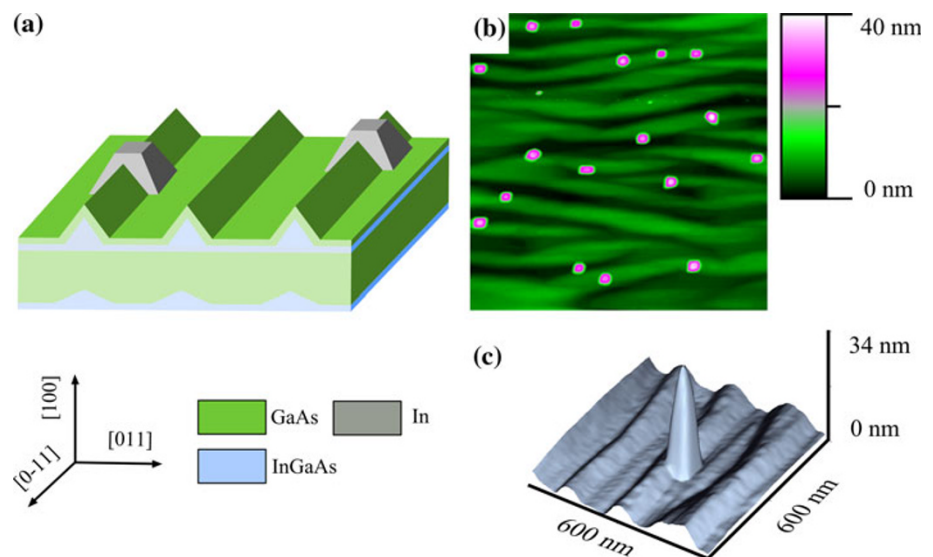
All samples were grown by solid-source MBE on undoped, singular GaAs (100) substrates following the procedure described in [13]. A 200-nm-thick GaAs buffer layer was grown after native oxide removal under  $\text{As}_4$  flux at 580°C. Next, a 15-period InGaAs/GaAs superlattice (SL) template was deposited to obtain 1D QD ordering on top [11]. Each

SL period consisted of a 2.3-nm  $\text{In}_{0.4}\text{Ga}_{0.6}\text{As}$  QD layer grown at 540°C and immediately capped with 0.7-nm GaAs, annealing for 2 min at 580°C, and a 12-nm GaAs layer grown at 580°C. On the SL template, a single layer of 2.3-nm  $\text{In}_{0.4}\text{Ga}_{0.6}\text{As}$  QDs was deposited that was capped with 3-nm GaAs. Afterward, the samples were cooled down to 120°C. During cooling down, the As valve was closed and In nanocrystals with 4 monolayers (ML) In amount were deposited at 120°C [14]. The growth rates for GaAs and InAs were 0.054 and 0.0375 nm/s. The morphology of the samples was characterized by a commercial tapping-mode atomic force microscope (AFM) under ambient conditions. PL measurements of the InGaAs QD arrays were taken in a He-flow cryostat. A frequency-doubled Nd/YAG laser (532 nm) was used as excitation source with excitation power density of 256 mW/cm<sup>2</sup>. The PL was dispersed by a single  $\frac{1}{4}$ -m monochromator and detected by a liquid-nitrogen-cooled InGaAs photodiode array. Additionally, low-temperature micro-PL measurements were taken in a similar setup with a 632.8-nm Helium–Neon laser excitation source using a long working distance, infinity-corrected microscope objective with numerical aperture of 0.5. The SPR of the In nanocrystals was measured by differential reflectivity (DR) spectroscopy [15] at room temperature. The setup consisted of a halogen lamp, a double  $\frac{1}{4}$ -m monochromator, and a PbS photodetector.

## Results and Discussion

The investigated structure is depicted in Fig. 1a. Due to multiple stacking and annealing, one-dimensional InGaAs QD arrays form due to the anisotropic properties of the GaAs (100) surface and strain-driven adatom migration

**Fig. 1** Schematic structure of the investigated sample (a). 2  $\mu\text{m}$  by 2  $\mu\text{m}$  AFM image of the investigated sample (b) and a magnified image of an individual In nanocrystal (c)



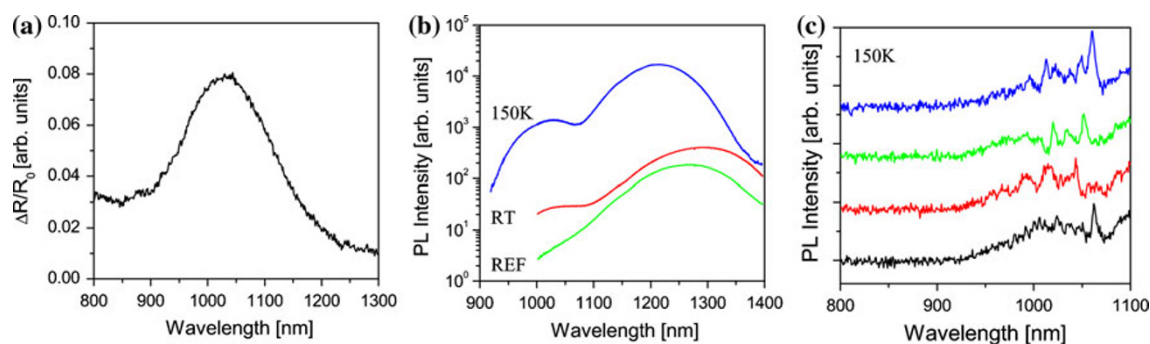


**Fig. 2** Differential reflectivity (a), PL (b), and micro-PL (c) spectra of the investigated sample. Different traces in c correspond to measurements taken at different positions on the sample

[11]. Deposition of In nanocrystals results also in their ordering on top of the QD arrays. It has been shown that the mechanism of In nanocrystal ordering is also strain-related [13]. This is justified by the fact that the ordering is preserved even after deposition of a thin GaAs capping layer, which radically smoothes the surface. Morphology-related ordering would be lost after capping, which is not the case as seen in Fig. 1b.

By choosing suitable deposition conditions, it is possible to obtain low densities of In nanocrystals, as seen in Fig. 1c. Such configurations are very promising for the investigation into coupled QD–SPR emission at the single QD level. It is well known that the SPR-related local field enhancement is extremely short-ranged [5], especially in high-index media like III-V semiconductors. Hence, only QDs that are in close proximity of an In nanocrystal can interact with its SPR. As a QD placed too close or too far away from the In nanocrystal either will be quenched or will not experience any effect from the SPR, the one-dimensional ordering of the QDs is very beneficial, because it implies that there always is a QD at the optimal distance from the In nanocrystal. Finally, a sufficiently low density of the In nanocrystals is necessary, so that there are only few of them in the laser spot, enabling observation of single QD–SPR coupling using standard micro-PL spectroscopy.

The results of the optical characterization of the investigated sample are presented in Fig. 2. DR measurements reveal a distinct peak due to the SPR of the In nanocrystals around 1  $\mu\text{m}$  (Fig. 2a). Tuning of the SPR into the near-infrared spectral region is most likely due to the high refractive index of GaAs and also the rather complicated shape of the In nanocrystals. Room-temperature PL reveals a clear emission peak centered around 1.25  $\mu\text{m}$  from the QD array (Fig. 2b). It has an additional feature in the 1  $\mu\text{m}$  region, which is attributed to coupled QD–SPR emission. No such feature is visible for the reference sample without In nanocrystals. It is also not observed for samples with thicker GaAs capping layer, indicating that the observed

effect is near-field-related. At lower temperature, the SPR-related peak becomes more pronounced, most likely due to lower resistive losses in the metal. Micro-PL measurements show that the SPR-related peak around 1  $\mu\text{m}$  is composed of sharp lines due to emission from individual QDs (Fig. 2c). No such splitting is resolved for samples without In nanocrystals as the QD density is too large. This evidences that only emission from single QDs close to the sparse In nanocrystals is enhanced, reconfirming that the enhancement is near-field-related. Hence, coupled QD–SPR emission at the single QD level is observed for the first time in an all solid-state system.

## Conclusions

To conclude, we demonstrated the alignment of In nanocrystals on one-dimensional InGaAs QD arrays formed by self-organized anisotropic strain engineering on GaAs (100) by MBE. The mechanism of In nanocrystal ordering is strain-driven. The SPR of the In nanocrystals leads to clear modification of the QD emission spectrum and the occurrence of an additional emission band coinciding with the SPR wavelength region. Low-temperature micro-PL measurements revealed that this band is composed of sharp lines due to emission from individual QDs, meaning that QD–SPR coupling was observed at the single QD level.

**Open Access** This article is distributed under the terms of the Creative Commons Attribution Noncommercial License which permits any noncommercial use, distribution, and reproduction in any medium, provided the original author(s) and source are credited.

## References

1. A. Badolato, K. Hennessy, M. Atature, J. Dreiser, E. Hu, P.M. Petroff, A. Imamoglu, *Science* **308**, 01158 (2005)
2. W. Chang, W. Chen, H. Chang, T. Hsieh, J. Chyi, T. Hsu, *Phys. Rev. Lett.* **96**, 0117401 (2006)

3. D. Englund, D. Fattal, E. Waks, G. Solomon, B. Zhang, T. Nakaoka, Y. Arakawa, Y. Yamamoto, J. Vučković, *Phys. Rev. Lett.* **95**, 0013904 (2005)
4. J.N. Farahani, *Phys. Rev. Lett.* **95**, 0017402 (2005)
5. O. Kulakovich, N. Strekal, A. Yaroshevich, S. Maskevich, S. Gaponenko, I. Nabiev, U. Woggon, M. Artemyev, *Nano. Lett.* **2**, 01449 (2002)
6. T. Hanke, G. Krauss, D. Träutlein, B. Wild, R. Bratschitsch, A. Leitenstorfer, *Phys. Rev. Lett.* **103**, 257404 (2009)
7. M. Noginov, G. Zhu, A. Belgrave, R. Bakker, V. Shalaev, E. Narimanov, S. Stout, E. Herz, T. Suteewong, U. Wiesner, *Nature* **460**, 01110 (2009)
8. M. Stockman, *J. Opt. A. Pure Appl. Opt.* **12**, 024004 (2010)
9. R.M. Stevenson, R.J. Young, P. Atkinson, K. Cooper, D.A. Ritchie, A.J. Shields, *Nature* **439**, 0179 (2006)
10. R.K. Kramer, N. Pholchai, V.J. Sorger, T.J. Yim, R. Oulton, X. Zhang, *Nanotechnology* **21**, 0145307 (2010)
11. T. Mano, R. Nötzel, G.J. Hamhuis, T.J. Eijkemans, J.H. Wolter, *J. Appl. Phys.* **95**, 0109 (2004)
12. T. Van Lippen, R. Nötzel, G. Hamhuis, J. Wolter, *J. Appl. Phys.* **97**, 044301 (2005)
13. A. Urbańczyk, G.J. Hamhuis, R. Nötzel, *Appl. Phys. Lett.* **96**, 0113101 (2010)
14. A. Urbańczyk, G.J. Hamhuis, R. Nötzel, *J. Appl. Phys.* **107**, 0014312 (2010)
15. R. Lazzari, S. Roux, I. Simonsen, J. Jupille, D. Bedeaux, J. Vlieger, *Phys. Rev. B* **65**, 0235424 (2002)